



# 1 The analysis of H/V curve from different ellipticity retrieval 2 technique for a single 3c-station recording.

3 Irfan Ullah<sup>1</sup>, Renato Luiz Prado<sup>1</sup>.

4 1.Departamento de Geofísica do Instituto de Astronomia, Geofísica e Ciências Atmosféricas

5 Rua do Matão, 1226 - Cidade Universitária São Paulo-SP - Brasil

6 *Correspondence to:* Irfan Ullah (syed\_528@yahoo.com)

7 **Abstract.** In the last two decades or so the H/V (Horizontal-to-Vertical Spectral Ratio) technique remained very popular,  
8 and are extensively used for the site fundamental frequency estimation. H/V curve are also used with dispersion curve to  
9 jointly invert and retrieved the shear wave velocity of relatively deep soil deposit. Although a full theoretical explanation of  
10 H/V technique is not been presented yet, There are two main assumptions used generally that H/V curves can be explained  
11 by considering Rayleigh wave of noise wave field only while the other newly presented approach utilized the whole noise  
12 wave field known as diffuse field approach (DFA), However in case of Rayleigh wave approach for H/V, it is almost  
13 impossible to the remove the fraction of Love wave to the horizontal component of H/V. Here in this study we aim to test  
14 different approaches adopted for the removal of Love wave fraction from horizontal component for a borehole test site at  
15 University of Sao Paulo. The result from different approaches are compared with borehole ellipticity curve. The result  
16 shows that around the fundamental frequency of curve obtained in either way(DFA or ellipticity approach) is dominated by  
17 Rayleigh waves.

18

## 19 **1. Introduction.**

20

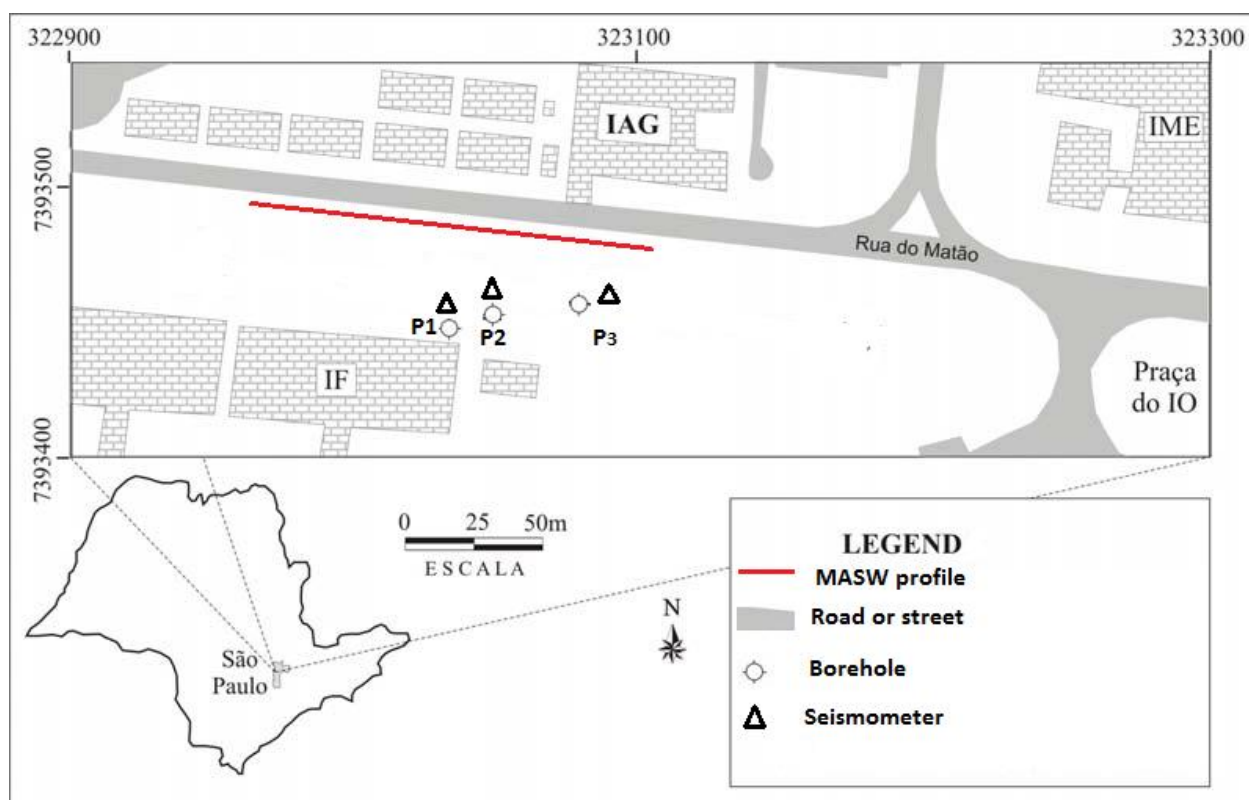
21 H/V (Horizontal-to-Vertical spectral ratio) is fast and quick way to get properties of a site for  
22 engineering interest, by the measurement of ambient noise wave field with a single 3-component sensor  
23 on the earth surface. The method is used for rapid estimation of fundamental resonance frequency ( $f_0$ )  
24 of a site where the maximum displacement amplification is expected in case of an earthquake. This  
25 technique is also used to retrieve the shear wave velocity of the geological structure in a joint inversion  
26 with dispersion curve (Scherbaum et al, 2003 Picozi et al, 2005 Hobiger et al, 2013). However, some  
27 controversies about the nature of ambient noise wave field and sources exist, which most of the time  
28 make the results of H/V curve questionable and hence debatable. Apart from the controversies exist in  
29 nature of ambient noise wave filed M. Mucciarelli et al (2001) described some problem regarding the



30 acquisition and processing of H/V spectral ratio. Due to extensive utilization of H/V technique, a  
31 commission was established to test the acquisition, processing and interpretation of this technique (site  
32 effects assessment using ambient excitations) – the SESAME project (2001-2004), The guidelines  
33 reports are published for acquisition, processing and interpretation of ambient noise wave field and have  
34 addressed all the points raised and discussed by M. Mucciarelli et al (2001) in extensive details. The  
35 H/V curve are modeled with different approaches and each modeling approach might have the effect on  
36 the retrieved soil profile(Sánchez-Sesma et al, 2011, Lunedei & Malischewsky 2015). The acquisition  
37 of the data is made with a three component sensor placed on the surface of ground which record the  
38 seismic noise wave field. Fourier spectra of the recorded seismic noise for all the three component (east-  
39 west , north-south and vertical) are made. The two horizontal component Fourier spectra are properly  
40 averaged and then divided by the vertical Fourier spectra. This division of averaged horizontal and  
41 vertical component result a curve (H/V) as function of frequency. H/V curve usually result a peak  
42 depending on the subsoil stratigraphical profile, this peak correspond to fundamental resonance  
43 frequency ( $f_0$ ) of the site (Tokimatsu, 1997; Bard, 1999; Bonnefoy-Claudet et al., 2006). The averaged  
44 horizontal component of H/V curve contain the contribution from both Rayleigh and Love wave and  
45 some fraction of body waves as well. In a joint inversion of H/V curve with dispersion curve this other  
46 elastic wave effect presence in the H/V curve might bias the retrieved s-wave velocity profile.  
47 Therefore, the presence of Love and other elastic waves existence in the H/V curve must be assumed or  
48 estimated before the inversion process (Bonnefoy-Claudet et al., 2006).Here in this communication we  
49 will try to list the different approaches used for the refining of H/V curve by removing unwanted  
50 fraction (Love wave effect presence) prior to the joint inversion with dispersion curve. At present there  
51 are two main research lines describing the H/V curve by taking in account the whole ambient-vibration  
52 wave field, and another just studies the surface wave and Rayleigh wave dominancy in noise wave field  
53 (Lunedei & Malischewsky 2015). Sánchez-Sesma et al (2011) proposed that seismic noise field can be  
54 consider as diffusion-like situation which contain all type of elastic wave (surface and body waves) . He  
55 suggested that the average autocorrelation of the motions at a given receiver, in the frequency domain,  
56 measures average energy density (DED) and is proportional to the imaginary part of the Green function  
57 (GF) when both source and receiver are the same. The surface wave dominancy opinion of noise wave



58 field is in favor of Rayleigh wave dominancy (Yamamoto, 2000 Boremann 2002, Cornou, 2002 ,  
59 Okada ,2003). We will try to check both these assumptions here with the borehole data.  
60 The site for which this analysis are made is a borehole site at university of Sao Paulo shown in Fig.1.  
61 The noise measurement were made with broadband 3 component seismometer nanometrics Trillium  
62 Compact 120-s. Ambient noise wave field measurements were made for 24 hours on weekend night to  
63 minimized cultural noise influence. The data acquisition of ambient noise has been done following the  
64 guidelines developed under the SESAME (2004) recommendations. To obtain the fundamental  
65 frequency of the site a window of one-hour recording were processed and the reliability condition  
66 proposed by SESAME (2004) for the H/V curve and peak were followed.



68 Fig. 1 shows the location map studied area ,legends explain the different symbols. (modified from Porsani 2004).  
69 We will try to discuss briefly here and analyzed our seismic noise data with this diffuse-field  
70 assumption (DFA). Later we will analyzed our data with assumption that H/V curve basically reflect the  
71 Rayleigh wave ellipticity.

72  
73 **2. Diffuse field assumption technique.**



74  
75 Sánchez-Sesma et al (2011) proposed to considered ambient noise wave field as diffuse wave field  
76 which contain all different types of waves (surface and body). The ambient noise wave field is  
77 generated by multiple random uncorrelated forces/sources near to or at the earth surface. The wave  
78 field may contain the scattering effect of various elastic mode. The field intensities could be in a better  
79 way described by diffuse like situation. To assume that the noise wave field is diffuse, the H/V curve  
80 can be estimated for a receiver at earth surface in term of green tensor imaginary part at the source  
81 (source and receiver are assumed to be at same location). The work of Sánchez-Sesma provides an idea  
82 of linkage between energy density and imaginary part of GF in 3D (energy densities of the noise wave  
83 field is proportional to the imaginary part of green tensor). The H/V curve obtained from the square  
84 root ratio of imaginary parts of GF (horizontal and vertical components) Eq.2 serve as intrinsic  
85 property of medium therefore its inversion can be used to retrieved subsurface soil profile. The detailed  
86 analysis of the method is beyond the scope of this communiqué, interested readers are referred to  
87 Sánchez-Sesma et al (2011) for detailed procedure. The summary of this procedure is that  
88 autocorrelation of motion at a receiver sensor in a given direction is proportional to directional energy  
89 density (DED), and this DED is proportional to the imaginary part of Green tensor at that sensor  
90 (Sánchez-Sesma et al 2011). Patron et al, (2009) showed that in case of 3D homogeneous elastic half  
91 space, the horizontal displacement (radial and transverse) have fix energy proportion (e.g  $E_1(x, x, \omega) =$   
92  $E_2(x, x, \omega)$  and also  $ImG_{11}(x, x, \omega) = ImG_{22}(x, x, \omega)$ ). For a diffused wave field the H/V can be  
93 represented in term of directional energy densities assuming source and receiver lies at same location  
94 ( $x$ ) on the surface of earth as

95

$$96 \frac{H}{V}(\omega) = \sqrt{\left( \frac{E_1(x, x, \omega) + E_2(x, x, \omega)}{E_3(x, x, \omega)} \right)} \quad (1)$$

97

$$98 \frac{H}{V}(\omega) = \sqrt{\left( \frac{ImG_{11}(x, x, \omega) + ImG_{22}(x, x, \omega)}{ImG_{33}(x, x, \omega)} \right)} \quad (2)$$

99 where in (1)

$$100 E_m(x, \omega) = \rho \omega^2 \langle u_m(x, \omega) u_m^*(x, \omega) \rangle \quad \text{where } m = 1, 2, 3$$

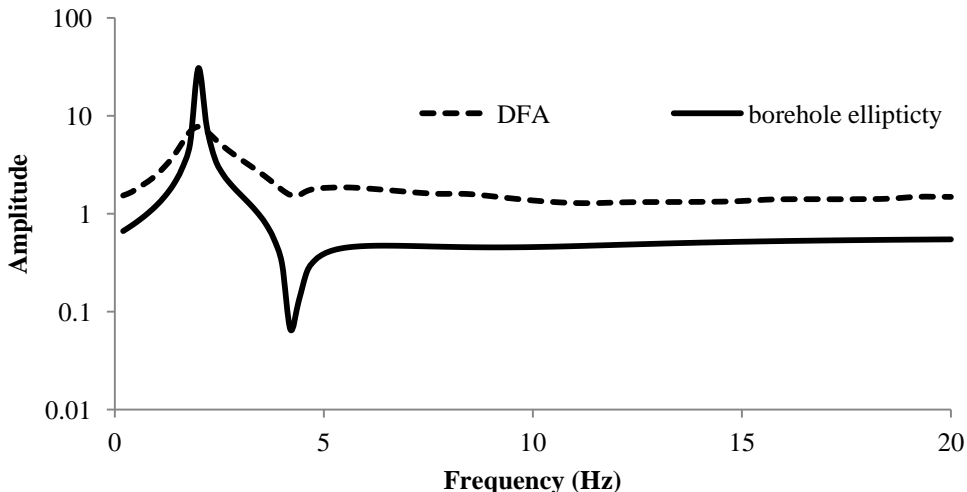
$$= -2\pi\mu E_s k_s^{-1} Im[G_{mm}(x, x, \omega)]$$



101 where energy density is find out at point  $x$  in direction  $m$ .  $\omega, \rho$  and  $u_m$  are angular frequency , layer  
102 density and displacement at point  $x$  respectively .  $E_s = \rho\omega^2s^2$  is the strength of diffuse illumination in  
103 term of shear wave average energy density  $\mu$  is shear wave modulus  $\langle \dots \rangle$  bracket shows the azimuthal  
104 average,  $k_s = \frac{\omega}{V_s}$  shear wave number  $V_s$  shows medium S-wave velocity. The symbol  $(^*)$  show complex  
105 conjugate process, the medium response in a direction  $m$  (of impulse load and acting in same direction)  
106 is indicated by  $G_{mm}$  .The H/V curve obtained in this manner are linked to the intrinsic property of  
107 medium , The resulted H/V curve from the diffuse-field approach might allow its inversion without  
108 considering any supplemented information (dispersion curve).  
109

110 For our analysis, the data of seismic noise recorded at borehole test site were analyzed with DFA  
111 (diffuse field assumption) frame work of Eq.2 ,  $\frac{H}{V}(\omega)$  result are obtained from the data with an  
112 integration step of 1000 and window length 40s.The curve obtained by this directional energy density  
113 approach is compared with borehole ellipticity Fig.2. The peak and trough of H/V curve obtained  
114 (Fig.2) correspond to peak and trough of ellipticity. However the shape of H/V curve is generally higher  
115 except the peak ,it is because of other elastic wave phases contribution. This peak and trough  
116 correlation of the H/V curve with borehole ellipticity shows that at these singularities ( peak and trough)  
117 Rayleigh wave contribution dominate the wave-field. It is important to note here the inversion of  
118 ellipticity curve with dispersion curve are recommended around the peak region of H/V curve (Picozi  
119 et al,2005 Hobiger et al, 2013). In next section we will focus our attention on the other line of research  
120 which is in the opinion of, that noise wave field is dominated by surface wave especially Rayleigh  
121 wave ( see section 3) , and H/V curve can be explained by its correlation with Rayleigh wave ellipticity  
122 curve (Bard 1999).  
123

124



125

126

127 Fig.2 H/V curve obtained through DFA technique at the test site (IAG-USP), the Borehole ellipticity curve is plotted in solid  
128 for comparison at the site.

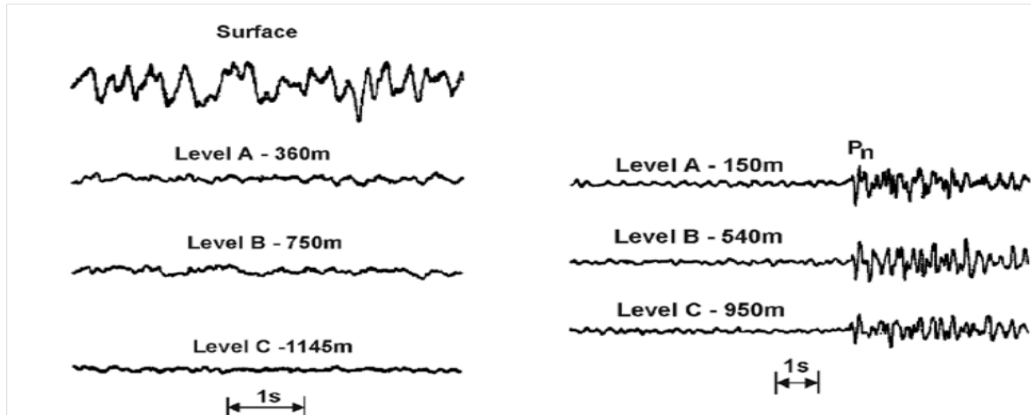
129

130 **3. Surface wave dominancy of seismic noise wave field.**

131

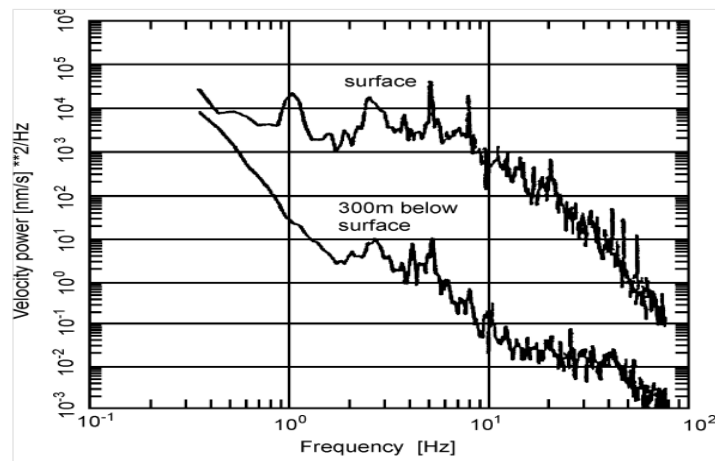
132 To find out that whether body or surface waves dominate the noise wave field is analyzed by Bormann  
133 (2002) , he used sensors for earthquake and seismic noise recording both at the surface and in the  
134 boreholes at different depth levels and concluded the surface-wave nature of seismic noise Fig. 3.  
135 Bormann (2002) showed that, the penetration depth of surface waves increases with wavelength, high  
136 frequency noise attenuates more rapidly with depth. In case of Fig.3 the noise power at 300 m depth in a  
137 borehole was reduced, as compared to the surface, by about 10 dB, at  $f = 0.5$  Hz, 20 dB at 1 Hz and 35  
138 dB at 10 Hz. This continuous amplitude decline with frequency is in accord with the surface waves  
139 nature of seismic noise.

140



141

142 Fig.3 Recording of seismic noise (left) and earthquake signals (right) at the surface and at different depth levels of a  
143 borehole. (Bormann 2002).



144

145 Fig. 4 Velocity power density spectra as obtained for noise records at the surface (top) and at 300 m depth in a borehole  
146 (below) near Gorleben, Germany (Bormann , 2002).

147 If the noise wave field is mainly dominated by surface wave then another question arise , that what is  
148 the fraction contribution of Rayleigh and Love waves to the noise wave field. Most of the researchers  
149 focused their attention to find the fraction Rayleigh to Love ratio from the analysis of noise wave field  
150 recorded on vertical component (Li et al., 1984; Horike, 1985; Yamanaka et al., 1994). The results of  
151 these studies showed an agreement in one aspect that microseism (<1Hz) are mainly dominated by  
152 Rayleigh waves however at high frequency (> 1Hz) a combination of P and Rayleigh wave exists

153

154 Table 1 summarize the result of previous studies on this issue.



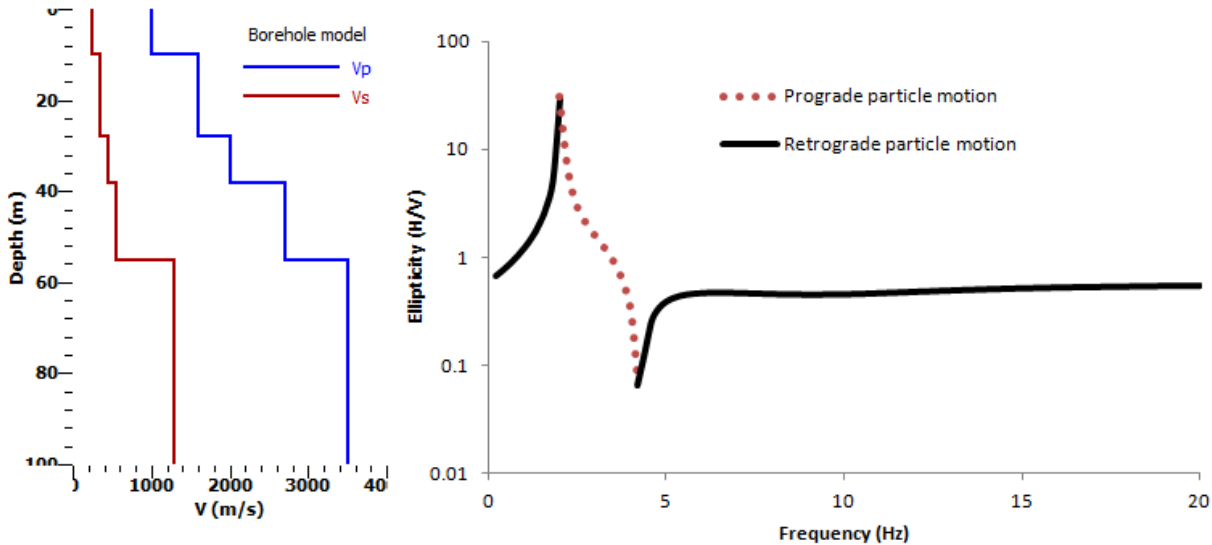
	Rayleigh waves(%)	Love waves(%)	frequency range(%)
<b>Chouet et al.,1998</b>	<b>30%</b>	<b>70%</b>	<b>&gt;2Hz</b>
<b>Yamamoto, 2000</b>	<b>&lt;50%</b>	<b>&gt;50%</b>	<b>3-10 Hz</b>
<b>Arai et al., 1998</b>	<b>30%</b>	<b>70%</b>	<b>1-12 Hz</b>
<b>Cornou, 2002</b>	<b>60%</b>	<b>40%</b>	<b>&lt; 1 Hz</b>
<b>Okada (2003)</b>	<b>&lt;50%</b>	<b>&gt;=50%</b>	<b>0.4-1 HZ</b>
<b>Köhler(2006)</b>	<b>10–35%</b>	<b>65–90%</b>	<b>0.5–1.3 Hz</b>

155

156 Table.1 Summary conclusions about the proportion of Rayleigh and Love waves in noise, after different authors (from  
 157 Chouet et al., 1998; Yamamoto, 2000; Arai et al. 1998; Cornou 2002, Okada 2003, Köhler2006 ).

158 **4.Removal of Love wave from horizontal component.**

159 Rayleigh wave are formed by the linear pairing of P (primary waves ) and Sv (vertically polarized  
 160 shear waves) waves (Aki, 2002).This pairing of vertical and horizontal components have a phase shift  
 161 of  $\pm \frac{\pi}{2}$  , the particle motion induced by Rayleigh wave will depict an ellipse, this elliptical motion will  
 162 either be retrograde or prograde depending on the sign of phase shift. Similarly Love wave is composed  
 163 of horizontally polarized shear waves (Sh). The horizontal over vertical axes of ellipse described by  
 164 particle motion under the Rayleigh wave influence is term as ellipticity. At situation of homogeneous  
 165 half-space the particle motion is retrograde at all frequencies and ellipticity is constant . However in  
 166 case of layered structure ellipticity exhibit a peak and trough and the particle motion switch from  
 167 retrograde to prograde and then to retrograde with the frequency, depending on the velocity contrast  
 168 between the soil and bedrock ( Konno and Ohmachi, 1998).



169

170

171 Fig.5 Borehole model at IAG-USP . The ellipticity curve of fundamental Rayleigh wave of the borehole model , marking the  
 172 frequency ranges where the retrograde and prograde motion might occur.

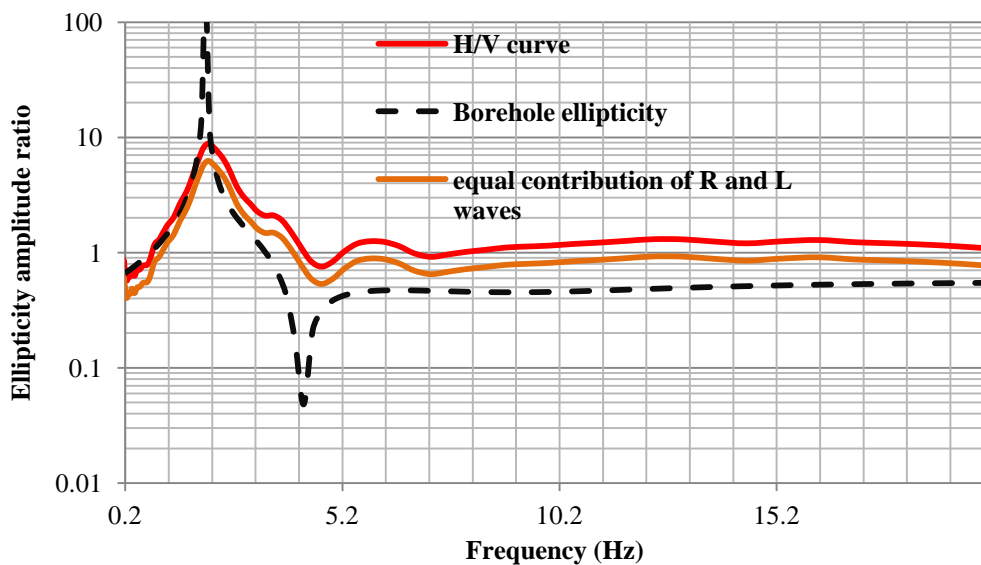
173

174 The conclusion from the preceding section can be drawn that, the contribution of Love wave to the  
 175 horizontal is not predictable and fluctuate with frequency and from site to site. The H/V are linked to  
 176 the ellipticity of Rayleigh wave , in situation where the high shear wave contrast exist between soil and  
 177 bedrock (Bard,1999).The H/V curve corresponds nicely to the peak of ellipticity curve (Fig.6). The  
 178 deviation between curves can be easily linked to the presence of Love wave contribution to noise wave  
 179 field at the horizontal component. We will try to review all the available technique for the this task and  
 180 compared its result with borehole ellipticity.

181 H/V curves are obtained and compared with the ellipticity curve of borehole at the same site. The  
 182 deviation between the curves are due to Love wave contribution. H/V curve is generally higher than the  
 183 ellipticity curve except at peak frequency of Rayleigh wave ellipticity Fig.6. Three different polarization  
 184 technique are used to minimized the effect of Love wave. The first technique is the simple H/V of  
 185 seismic noise (Fig.6) , In this technique the polarization mean the division of Fourier spectral amplitude  
 186 of averaged horizontal component over vertical component with the assumption that around the  
 187 fundamental resonance frequency the vertical component is dominated by Rayleigh only. Generally it is



188 believed that Rayleigh (P-Sv) and Love wave (Sh) contribute equally to the horizontal component. Fäh  
189 et al (2001) proposed the division of H/V spectral amplitude by  $\sqrt{2}$  for Love wave effect minimization  
190 from horizontal component Fig.6. However this is not a wise approach because the energy partition of  
191 horizontal component between Rayleigh and Love is not constant and varies with frequency and site  
192 (Köhler *et al.* 2006; Endrun 2011) Table 1. There are two other polarization approaches employed for  
193 this job recently are: time-frequency analysis (Fah *et al.* 2009) and RayDec (Hobiger *et al.*, 2009)  
194 followed by a concise introduction , the interested readers are referred for detail of these approaches  
195 (Fah *et al.* 2009) and (Hobiger 2009).



196  
197 Fig.6 shows the comparison of H/V curve of experimental data recorded at test borehole site at university of Sao Paulo.  
198  
199 **5. Time-frequency analysis.**  
200  
201 In time-frequency analysis the vertical component of noise wave field are considered as a trigger and its  
202 energy level are estimated at given time and frequency and are correlated with horizontal components  
203 (east-west , and north- south). A brief description of the technique is that continuous wavelet  
204 transformation (CWT) are performed on the eastern e(t) , northern n(t) and vertical v(t) components of  
205 noise wave field. CWT (continuous wavelet transform) transform a signal to time-scale plane. The  
206 scale is a single parameter which controls both the duration and bandwidth.CWT is defined as.

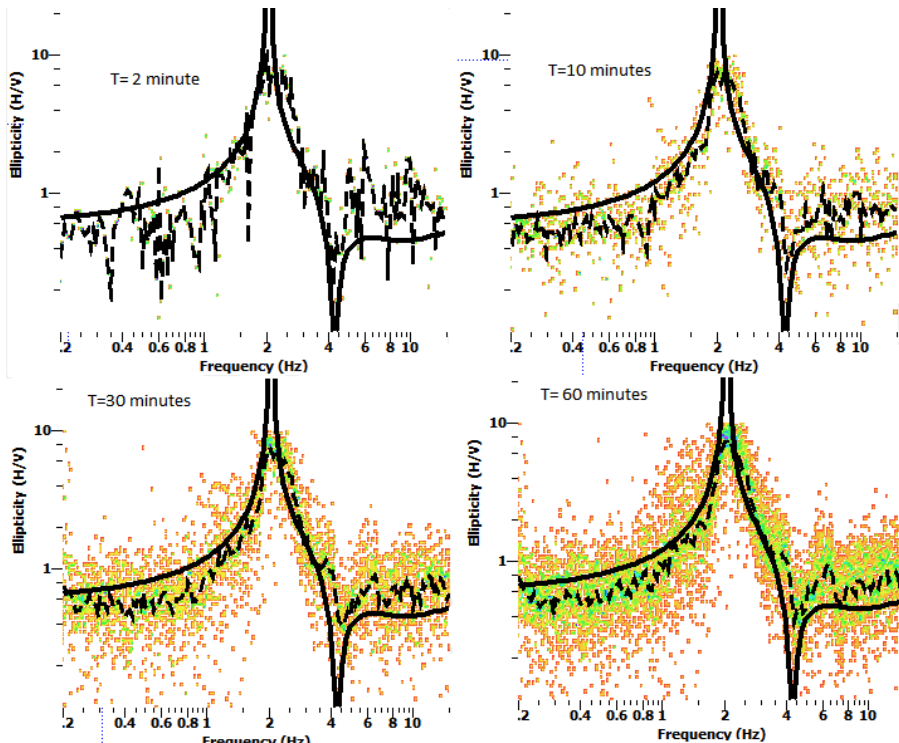


207 
$$\text{CWT}_{x(t)}(a, b) = \frac{1}{\sqrt{a}} \int_{-\infty}^{\infty} x(t) \psi^* \left( \frac{a-b}{a} \right) dt \quad (3)$$

208 where  $x(t)$  is real-valued signal component {where  $x(t) = e(t)$  or  $n(t)$  or  $v(t)$  },  $\psi(t)$  shows the mother  
 209 wavelet,\* shows a complex conjugation process, a scale parameter (scale control both the duration and  
 210 bandwidth)  $b$  is translation in time. Fah et.al ( 2009) used a modified Morelet wavelet in a code written  
 211 for this job due the reason that traditional Morelet wavelet does not act well for H/V analysis. The  
 212 modified Morelet transform is defined as

213 
$$\psi(t) = \exp(i2\pi ft) e^{\left(\frac{-t^2}{m}\right)} \quad (4)$$

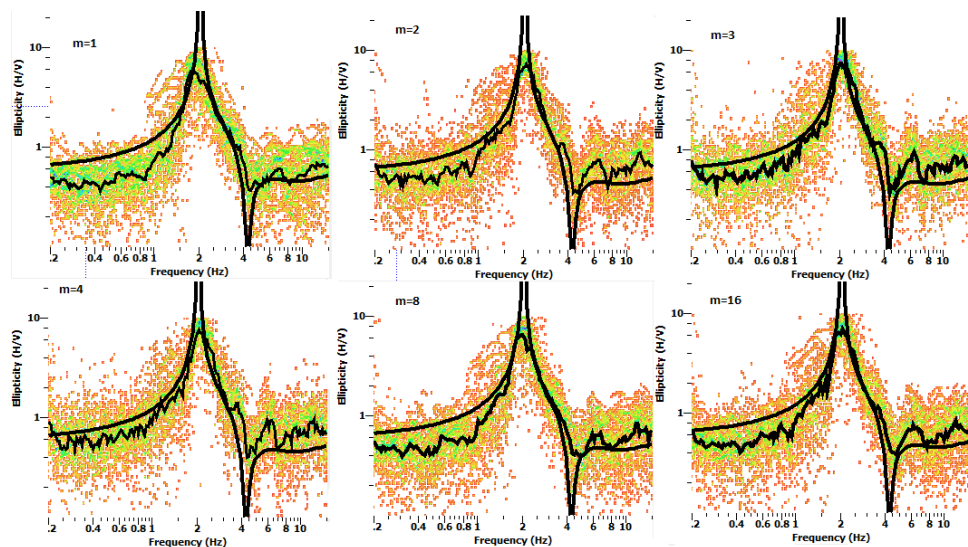
214 here  $f$  is the central frequency of the wavelet,  $m$  control the resolution of both frequency and time, low  
 215  $m$  mean more time localization on the expense of frequency resolution and higher  $m$  result on the  
 216 contrary i.e increase frequency resolution at the expense of time resolution. The classical Morelet  
 217 wavelet is achieved when  $m=1/2$ . After the application of CWT to each component of a single 3-c  
 218 sensor recording {  $e(t), n(t)$  or  $v(t)$  } give rise to three signals amplitude which is both the function of  
 219 time and frequency. Two horizontal ( $e(t), n(t)$  ) component are merged together to a single component.  
 220 As Rayleigh wave are the result of the coupling of p and vertically polarized S-waves, The vertical  
 221 component is sorted out for amplitude maxima at each frequency and time translation . Similarly, the  
 222 horizontal component is analyzed for amplitude maximum at given frequency and time, the horizontal  
 223 components are phase shifted  $\pm$  at a quarter of the period. This shift of period is done because of  
 224 theoretical phase shift between  $\pm\frac{\pi}{2}$  vertical and horizontal component particle motion. For each  
 225 maximum on the vertical component, the corresponding maximum on the horizontal component are  
 226 stored and the ratio of H/V are estimated. There is only one tuning parameter  $m$  ,the effect of its  
 227 different values of  $m$  are shown in Fig.8 , Also the effect on the length of the recorded signal is shown  
 228 in Fig.7. This whole process is statistically analyzed by histogram for all the frequency and translation  
 229 of time and H/V is obtained by the maximum of each histogram. For detail theoretical outline of this  
 230 analysis please read (Fah et.al, 2009).



231

232 Fig.7 Ellipticity (H/V) obtained from continuous wavelet transformation CWT for different length of the recorded signal; a  
 233 histogram is drawn for each frequency, the color within histogram indicates the energy level. (dashed line shows ellipticity  
 234 obtained from CWT while solid line shows the ellipticity curve obtained from borehole data at same location - IAG-front)

235



236



237

238 Fig.8 Ellipticity (H/V) obtained from continuous wavelet transformation CWT for different value of m; (curvy line shows  
239 ellipticity obtained from CWT while solid line shows the ellipticity curve obtained from borehole data at same location -  
240 IAG-front)

241

242 Fig.7 and 8 show a better result when compared with the borehole ellipticity curve of borehole. The  
243 result of wavelet transform Fig.7&8 shows that the ellipticity of borehole is retrieved in better way( especially at right limb of the ellipticity) when the recorded length of the signal is greater than 30  
244 minute ,and when the value of  $m \geq 8$ .

245

246

## 247 **6 Random decrement technique (RAYDEC).**

248

249 Another polarization technique use for the effect of Love (Sh) wave effect minimization for a single 3  
250 component sensor recording is term as RayDec technique (Hobiger et.al, 2009) The vertical component  
251 is taken as master trigger as because the Sv arrival occur only on the vertical component, while stacking  
252 a large number of horizontal component to obtained ellipticity of Rayleigh curve (Hobiger et al., 2009)  
253 showed that the obtained ellipticity will be closer to the true ellipticity curve rather than the H/V curve.

254 To elaborate RayDec techniques consider a signal {where  $x(t) = e(t)$  or  $n(t)$  or  $v(t)$  }. These three  
255 time series has  $N$  number of data points and having length  $T$ . To obtain a Rayleigh wave ellipticity  
256 curve, the main idea of this method is to obtain only Rayleigh waves in comparison of other waves type  
257 by the addition of a large number of filtered signal windows  $\Delta$ , estimates the energy level of horizontal  
258 averaged and vertical signal in a location where the vertical component change its sigh from -ve to +ve.

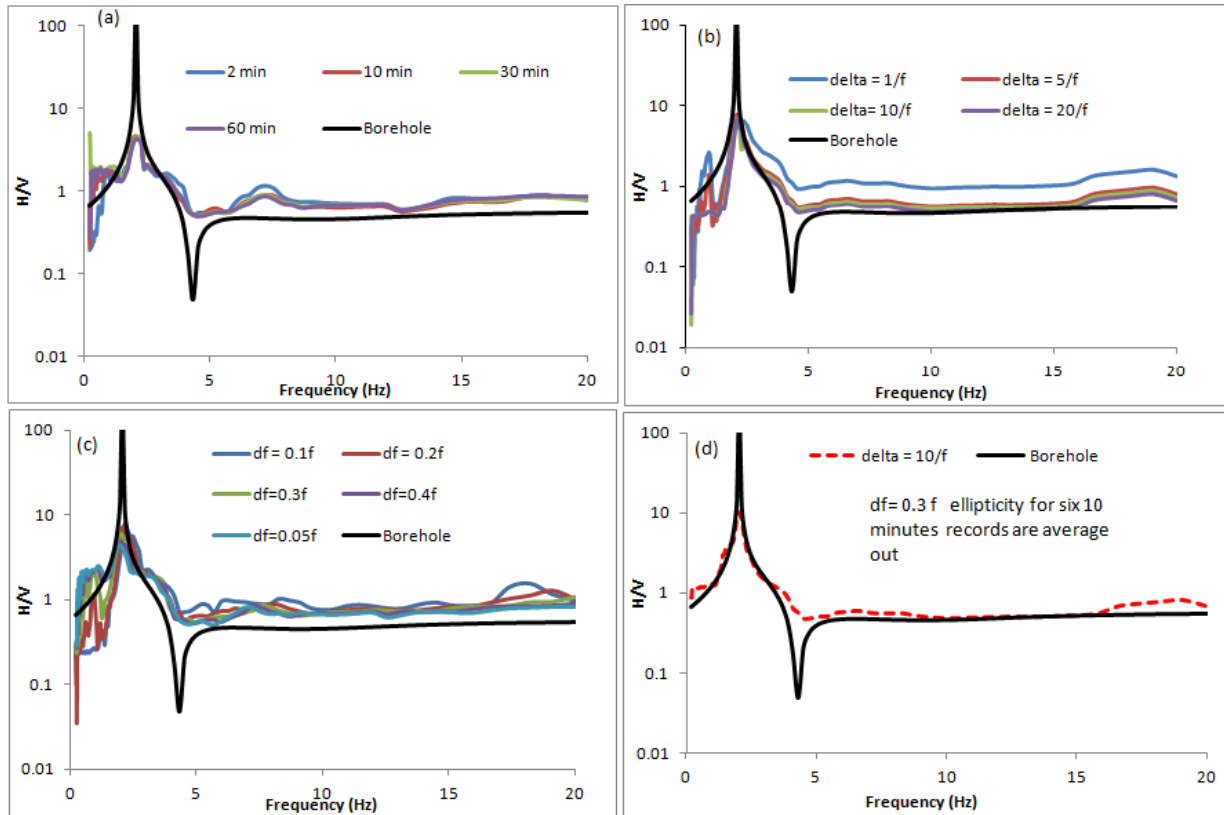
259 Due to the phase shift of  $\frac{\pi}{2}$  between Rayleigh wave vertical and horizontal component, both the  
260 horizontal component of EW and NS are projected by factor  $\phi$  with north direction in such a way to  
261 maximized the correlation between the summed horizontal and vertical component. The Rayleigh wave  
262 ellipticity is obtained latterly from Eq.5 . The ellipticity  $E$  is calculated as the square root of the ratio of  
263 the energies in the signal window.  $\Delta$ .

264 
$$E = \sqrt{\frac{\int_0^{\Delta} hf^2 \cdot s(t) \cdot dt}{\int_0^{\Delta} vf^2 \cdot s(t) \cdot dt}} \quad (5)$$



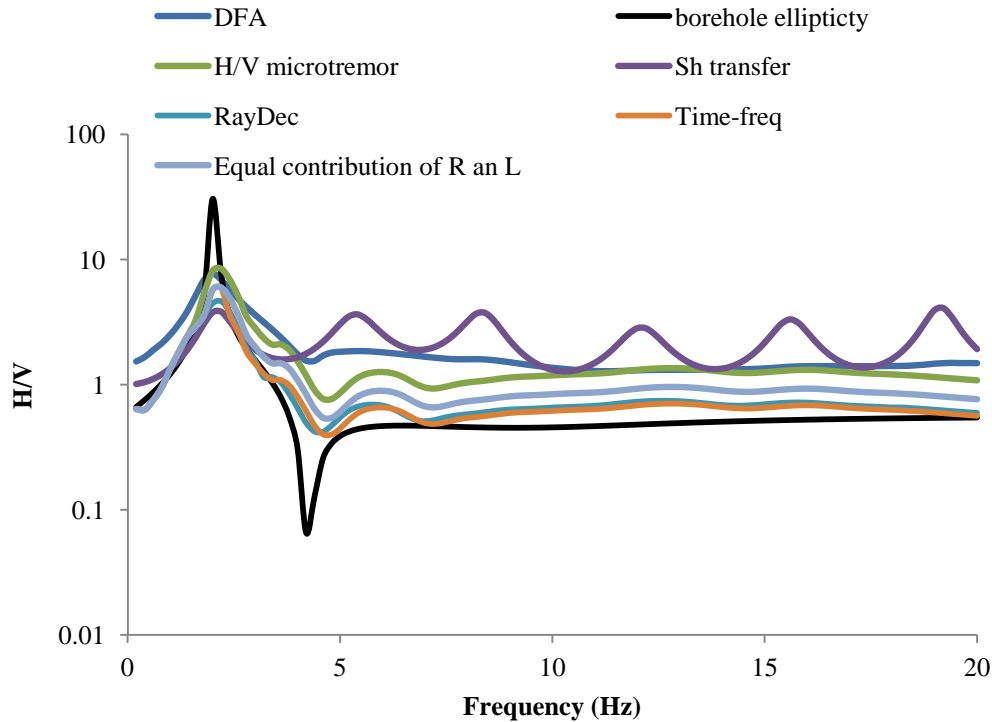
265 where  $hf.s(t)$  is the horizontal average ( NS north-south , EW east-west) signal and  $Vf.s(t)$  is the  
266 vertical component. This process is repeated for a whole record for an increment of window length  $\Delta$   
267 .The window length is taken as function of frequency such that to ensure 10 significant cycle at chosen  
268 frequency ( $\Delta=10/f$  where  $f$  is the analyzing frequency from 0.2 to 20 Hz are used). There are two tuning  
269 parameter for this technique ,  $\Delta$  (window length) and  $df$  (width of frequency filter). The effect of these  
270 two tuning parameter on the result is shown Fig.9. For our analysis we used one-hour records of noise,  
271 which were divided into 6 segments of 10 minutes each , afterward, the result is average out for all the  
272 six segments with the aim for minimization of misfit (see for detail procedure Hobiger et al., 2009). The  
273 result of ellipticity obtained via RayDec show a better match with borehole curve especially at right and  
274 left limb.  
275 The analysis of both time-frequency and RayDec for H/V give satisfactory result for the ellipticity  
276 retrieval of Rayleigh waves. Fig 10 shows the comparison of all the technique retrieved curves with that  
277 of borehole ellipticity.

278



279  
 280

281 Fig.9 Ellipticity obtained via RADEC technique , (a) shows the effect signal duration on the result.(b) shows the effect of  
 282 using different width of window (c) shows the effect of different filter width on the result (d) shows six 10-minute windows  
 283 (ellipticity for each 10 minute is obtained at the end the result is average and compared with borehole data black line).



284  
 285      Fig.10 Show the comparison of borehole ellipticity curve combine with that of all ellipticity retrieval technique.

286 **7.Discussion and conclusion.**

287 Deep soil shear wave velocity information can be retrieved from the joint inversion of H/V curve with  
 288 dispersion curve. The H/V curve are assumed to be linked with Rayleigh wave ellipticity for a site.  
 289 However in real situation the H/V curve technique can not completely replicate the Rayleigh wave  
 290 ellipticity. It is because of the presence of different elastic wave influence presence in the H/V curve  
 291 retrieval. Diffuse field approach is a better way to consider the effect of all elastic seismic phases (body  
 292 and surface wave). However the analysis of our data shows that at singularities (peak and trough)  
 293 especially at peak of the H/V curve obtained via DFA is very well correlated with Rayleigh ellipticity  
 294 curve in term of these singularities frequency. This matching can be assumed that around the peak  
 295 frequency even in case of diffuse like field situation the seismic noise field is dominated surface wave  
 296 especially Rayleigh waves.

297 The other approach used for the H/V curve technique is linked to the surface wave dominancy  
 298 especially Rayleigh wave around the singularities. Three different polarization technique for retrieval of



299 ellipticity curve by minimizing the Sh contribution to the horizontal component are simple H/V with  
300 equal contribution of Rayleigh and Love wave, time-frequency analysis and RayDec technique. The  
301 result of equal assumption of Rayleigh/Love wave fraction is unable to match with parts of borehole  
302 ellipticity except at peak. However ellipticity curve retrieved from noise analysis through time-  
303 frequency and RayDec shows a good replication of borehole ellipticity around the peak, right and left  
304 limb.

305 For the deep soil deposit the joint inversion of ellipticity and dispersion curve of Rayleigh wave are  
306 recommended. However due to the presence of effect of other seismic elastic phases especially Love  
307 wave may produced some bias result. Therefore it is extremely necessary to retrieved a H/V curve  
308 where the effect of Love wave contribution are minimized prior to the inversion with dispersion curve.  
309 For our test site we found that time-frequency and RayDec show better result ,by replication left and  
310 right limb of ellipticity curve of the borehole at the site.

### 311 **Acknowledgement.**

312 We are thankful to the Sanchez-Sesma (Instituto de Ingeniería Universidad Nacional Autónoma de  
313 México) for sharing his code for DFA analysis of seismic noise. We appreciate the help from of  
314 Hobiger (ETH Zurich) and Marc Wathelet (University Joseph Fourier - Grenoble 1, Grenoble) . We are  
315 indebted to Marcelo Assumpcao, Galiardo , Felipe Neves (Instituto de Astronomia, Geofísica e  
316 Ciências Atmosféricas, university of Sao Paulo) for providing the instruments for recoding and  
317 technical assistance. This work is completed with help of TWAS-CNPq for fellowship grant number  
318 190038/2012-8 (CNPq/TWAS - Full-Time Ph.D. Fellowship - GD 2012 ) for financial support.

319

### 320 **References:**

321 [1]. Aki, K., and P.G. Richards. : Quantitative seismology, Second Edition, University Science Books.**2002**  
322 [2]. Arai, H., and K. Tokimatsu. : Evaluation of local site effects based on microtremor H/V spectra. Proceeding  
323 of the Second International Symposium on he Effects of Surface Geology on Seismic Motion. Yokohama,  
324 Japan.**2** 673-680, **1998**.  
325 [3]. Bard, P.Y.: Microtremor measurements: a tool for site effect estimation?. The Effects of Surface Geology  
326 on Seismic Motion, eds. K. Irikura, K. Kudo, H. Okada and T. Sasatani (Balkema, Rotterdam), 1251-1279,  
327 **1999**.  
328 [4]. Bonnefoy-Claudet, S., Cornou, C., Bard, P.-Y., Cotton, F., Moczo, P., Kristek, J. & F'ah, D., 2006a. : H/V  
329 ratio: a tool for site effects evaluation. Results from 1-D noise simulations, *Geophys. J. Int.*, 827–837, **2006**.



330 [5]. Bormann, P. NMSOP – New Manual of Seismological Observatory Practice. IASPEI.  
331 GeoForschungsZentrum Potsdam, Germany. **2002**.

332 [6]. Chouet, B., De Luca, G., Milana, G., Dawson, P., Martini, M., Scarpa, R. : Shallow velocity of Stromboli  
333 volcano, Italy, derived from small-aperture array measurements of Strombolian tremor. Bull. Seism. Soc.  
334 Am., 88-3, 653-666, **1998**.

335 [7]. Cornou, C. Traitement d'antenne et imagerie sismique dans l'agglomération grenobloise (Alpes françaises):  
336 implications pour les effets de site (In french). Université Joseph Fourier, 260, **2002**.

337 [8]. D. Fäh, M. Wathelet, M. Kristekova, H. Havenith, B. Endrun, G. Stamm, V. Poggi, J. Burjanek, and C.  
338 Cornou. : Using ellipticity information for site characterisation. NERIES deliverable JRA4 D4. [Online].  
339 Available: <http://www.neries-eu.org>, **2009**.

340 [9]. Endrun, B. : Love wave contribution to the ambient vibration H/V amplitude peak observed with array  
341 measurements, J. Seismol., 15, 443–472, **2011**.

342 [10]. Enrico Lunedei and Peter Malischewsky A. Ansal (ed.). : Perspectives on European Earthquake  
343 Engineering and Seismology, Geotechnical, Geological and Earthquake Engineering 39, DOI 10.1007/978-  
344 3-319-16964-4\_15, **2015**.

345 [11]. Hobiger, M., P.-Y. Bard, C. Cornou, and N. Le Bihan . : Single station determination of Rayleigh wave  
346 ellipticity by using the random decrement technique (RayDec), Geophys. Res. Lett., 36, L14303,  
347 doi:10.1029/2009GL038863, **2009**.

348 [12]. Horike, M. : Inversion of phase velocity of long period microtremors to the S-wave-velocity structure  
349 down to the basement in urbanized areas. J. Phys. Earth, 33, 59-96, **1985**.

350 [13]. Jorge Luís Porsani , Weliton Borges, Wagner Roberto Elis , Liliana Alcazar Diogo . :  
351 Investigações geofísicas de superfície e de poço no sítio controlado de geofísica rasa do IAGUSP, Revista  
352 Brasileira de Geofísica. **2004**.

353 [14]. Kohler, A., Ohrnberger, M. & Scherbaum, F. : The relative fraction of Rayleigh and Love waves in  
354 ambient vibration wavefields at different European sites, in Proceedings of the 3rd Int. Symp. on the Effects  
355 of Surface Geology on Seismic Motion, Grenoble, 30 August–01 September, Vol. 1, pp. 351–360, **2006**.

356 [15]. Konno, K., and T. Ohmachi . : Ground-Motion Characteristic Estimated from Spectral Ratio between  
357 Horizontal and Vertical Components of Microtremor. Bull. Seism. Soc. Am., 88, 228-241, **1998**.

358 [16]. Li, T. M. C., Ferguson, J. F., Herrin, E., D. H. B. : High-frequency seismic noise at Lajitas, Texas. Bull.  
359 Seism. Soc. Am. **74-5**, 2015-2033, **1984**.,

360 [17]. M. Hobiger,, C. Cornou,1 M. W athelet,G. Di Giulio,B. Knapmeyer Endrun, F. Renalier,P.-Y. Bard,1 A.  
361 Savvaidis, S. Hailemikael,N. Le Bihan,M. Ohrnberger and N. : The Ground structure imaging by inversions  
362 of Rayleigh wave ellipticity sensitivity analysis and application to European strong-motion sites Geophys. J.  
363 Int. 192, 207–229. **2013**.

364 [18]. Mucciarelli M. and Gallipoli M.R. : A critical review of 10 years of microtremor HVSR technique. Boll.  
365 Geof. Teor. Appl., 42, 255-266, **2001**.

366 [19]. Okada, H. : The Microtremor Survey Method. Geophys. Monograph Series, SEG, 129 pp, **2003**.

367 [20]. Perton, M., Sánchez-Sesma, F.J., Rodríguez-Castellanos, A., Campillo, M. & Weaver, R.L. : Two  
368 perspectives on equipartition in diffuse elastic fields in three dimensions, J. acoust. Soc. Am., 126(3), 1125–  
369 1130, **2009**.

370 [21]. Picozzi, M., Parolai, S., Richwalski, S.M. : Joint inversion of H/V ratios and dispersion curves from  
371 seismic noise: Estimating the S-wave velocity of bedrock. Geophys. Res. Lett., 32, No.11doi:  
372 10.1029/2005GL022878

373 [22]. Sanchez-Sesma, F.J. : A theory for microtremor H/V spectral ratio: application for a layered medium,  
374 *Geophys. J. Int.*, **2011**, 186(1), 221–225, **2005**.



375 [23]. Scherbaum, F., K.-G. Hinzen, and M. Ohrnberger, : Determination of shallow shear-wave velocity  
376 profiles in Cologne, Germany area using ambient vibrations. *Geophys. J. Int.* 152, 597-612, **2003**.  
377 [24]. SESAME scientific products at [http://SESAME.geopsy.org/SES\\_Reports.htm](http://SESAME.geopsy.org/SES_Reports.htm), **2001-2004**  
378 [25]. Tokimatsu, K. : Geotechnical site characterization using surface waves. *Earthquake Geotechnical  
379 Engineering*, Ishihara (ed.), Balkema, Rotterdam, 1333-1368, **1997**.  
380 [26]. Yamamoto, H. (2000). : Estimation of shallow S-wave velocity structures from phase velocities of love-  
381 and Rayleigh- waves in microtremors. *Proceedings of the 12th World Conference on Earthquake  
382 Engineering*. Auckland, New Zealand, **2000**.  
383 [27]. Yamanaka, H., Takemura, M., Ishida, H., Niwa, M. : Characteristics of long-period microtremors and their  
384 applicability in exploration of deep sedimentary layers. *Bull. Seism. Soc. Am.* 84, 1831-1841, **1994**.  
385